Seasonal variability of cloud optical depth over northwestern China derived from CERES/MODIS satellite measurements

Yonghang Chen (陈勇航)[1], Hongtao Bai (白鸿涛)[1], Jianping Huang (黄建平)[2], Hua Zhang (张 华)[3], Jinming Ge (葛觐铭)[2], Xiaodan Guan (管晓丹)[2], and Xiaoqin Mao (毛晓琴)[1]

[1] *College of Environmental Science and Engineering, Donghua University, Shanghai 201620*

[2] *College of Atmospheric Sciences, Lanzhou University, Lanzhou 730000*

[3] *National Climate Centre of China Meteorological Administration, Beijing 100081*

Received November 13, 2007

The seasonal variability of cloud optical depth over northwestern China derived from Clouds and the Earth's Radiant Energy System (CERES) Single Scanner Footprint (SSF) Aqua Moderate Resolution Imaging Spectroradiometer (MODIS) Edition 1B data from July 2002 to June 2004 is presented. The regions of interest are those with Asia monsoon influence, the Tianshan and Qilian Mountains, and the Taklimakan Desert. The results show that the instantaneous measurements presented here are much higher than the previous results derived from International Satellite Cloud Climatology Project (ISCCP) D2 monthly mean data. Generally the measurements of cloud optical depth are the highest in summer and the lowest in winter, however, Taklimakan Desert has the lowest measurements in autumn. The regional variation is quite significant over northwestern China.

OCIS codes: 280.0280, 280.1310, 010.0010, 010.3920, 120.0120.

Clouds are the key regulator of the planet's climate by absorbing and reflecting solar radiation, and absorbing and emitting thermal radiation. Nowadays with the advent of satellite platforms that are regarded as the most efficient and reliable means of fulfilling cloud observational requirements, scientists have utilized optical theories to detect and retrieve cloud parameters[1−9]. For example, Liou *et al.* developed a methodology to retrieve three-dimensional ice water content and mean effective ice crystal size of cirrus clouds based on the retrieval of cloud optical depth (OD)[1]. Hu *et al.* studied CALIPSO lidar multiple scattering and depolarization for clouds[2,3]. Zhang *et al.*, Yang *et al.*, and Yuan *et al.* found improved algorithms for cloud detection[4−6]. A knowledge of cloud properties is crucial to the understanding of cloud's impact on the climate and environment change[7−9]. In China, Yi *et al.*[10], Chen *et al.*[11], Liu *et al.*[12], and Ding *et al.*[13] analyzed the spatial distribution and temporal variation of cloud amount over northwestern China, the whole China or global, using the data of International Satellite Cloud Climatology Project (ISCCP). Their results are helpful to a better understanding of clouds, however, cloud OD has been rarely addressed.

OD is a general measure of the capacity of a cloud to prevent the passage of light. Greater OD means greater blockage of the light and a larger cooling of the Earth-atmosphere system. According to the previous research[15−17], the spectral OD for a given particle size distribution over some distance is

$$\tau_\lambda = \pi Q_\mathrm{e} \int_{Z1}^{Z2} N r_\mathrm{e}^2 \mathrm{d}Z, \tag{1}$$

where Q_e is the extinction efficiency, and the effective radius is

$$r_\mathrm{e} = \frac{\int_{r1}^{r2} r\pi r^2 n(r)\mathrm{d}r}{\int_{r1}^{r2} \pi r^2 n(r)\mathrm{d}r}, \tag{2a}$$

$n(r)$ is the number density of droplets with radius r, and N is the total particle number density. To distinguish between water and ice clouds, r_e will be used for water clouds and the equivalent diameter

$$D_\mathrm{e} = \frac{\int_{L1}^{L2} D(L)\pi A_\mathrm{e}(L)n(L)\mathrm{d}L}{\int_{L1}^{L2} \pi A_\mathrm{e}(L)n(L)\mathrm{d}L} \tag{2b}$$

will be used for ice clouds. The variable $D(L)$ is the volume equivalent diameter of the hexagonal ice crystal of length L and width d. It is assumed that there is a monotonic relationship between L and d for the hexagonal ice columns defined by Takano and Liou[14], and this yields a unique relationship between the cross-sectional area A_e of these randomly oriented columns and L[15].

τ_e, r_e or D_e, and other cloud parameters affect the radiation absorbed, reflected, transmitted, and emitted by a given cloud. The dependence of the radiation field on these variables can be simulated using radiative transfer calculations. Cloud effective particle size, OD, phase, and cloud temperature can be determined from satellite-measured multispectral radiances by matching the radiances to the computed radiative transfer results[15−17].

In the visible portion of the spectrum, the cloud OD is almost entirely due to scattering by droplets or crystals, and ranges through orders of magnitude from low values less than 0.1 for thin cirrus to over 1000 for a large cumulonimbus and so should be primarily measured. Tselioudis *et al.*[18] and other scentists[10−13] studied OD estimates from ISCCP and found the cloud distribution takes on remarkable regional features. But the resolution of ISCCP dataset is not sufficient to probe detailed differences of clouds among relatively smaller sub-regions so that recently scientists use new generation of sensors such as the Moderate Resolution Imaging Spectroradiometer (MODIS) to study cloud optical properties, for example, Minnis *et al.*[7], Meyer *et al.*[8], Fu *et al.*[9] and other scientists[15−17,19,20] have addressed the topics. In this letter, we utilize the Single Scanner Footprint (SSF) MODIS Edition 1B data onboard Aqua satellite from July 2002 to June 2004, lately released from Clouds and the Earth's Radiant Energy System (CERES)[15]. The dataset is performed using 1-km MODIS pixels sampled to a 4-km resolution instead of taking one $4 - 10$ km pixel in each 30 km by 30-km box as in ISCCP. Regional cloud type frequencies derived for $1° \times 1°$ latitude-longitude-equal-area regions are used to determine cloud type frequencies of occurrence over the entire 60S—60N domain[20]. Thus it can meet the requirement of characterizing the cloud properties over sub-regions in northwestern China that has various topographies such as deserts, mountains, and oases in a large territory of about 4,290,000 km^2.

The CERES cloud detection algorithm is more advanced than the global cloud datasets (e.g. ISCCP) in that it uses four instead of two wavelengths to decide whether a given pixel is clear or cloudy[20]. Radiance measurements at these four wavelengths are used to estimate cloud OD[15−17]. One of the major optical advances of the CERES is the ability to use high spectral and spatial resolution cloud imager data to determine cloud and surface properties within the relatively large CERES field of view (20-km diameter for Aqua)[16]. Another advantadge is that the SSF incorporates new CERES angular distribution models (ADMs) based on improved scene identification to obtain more accurate fluxes at top of atmosphere from satellite-measured radiances. Those optical advances allow the CERES cloud data with unprecedented accuracy[15−17].

In this letter, the seasonal means are calculated for three-month seasons (e.g. winter is defined as December, January, and February). We will also demonstrate the annual cycle by calculation of individual monthly means. The yearly mean is computed as the average of four seasons. The statistics are based on a 1° latitude by 1° longitude grid in which pixel data are binned and averaged.

The SSF products include the cloud OD for up to two cloud layers defined as lower and upper layer. We derived the spatial distribution of cloud OD by averaging the available data for each day from July 2002 to June 2004. Figure 1 shows that the measurements of OD for lower layer clouds range from 4 to 23 and for upper layer clouds range from 3 to 18; the lowest measurements are over Gurbantunggut, Taklimakan, Badainjaran, and Tengger deserts. For both lower and upper layer clouds, the mountain regions have relatively high measurements of OD but not the highest; the highest measurements are over the Asia monsoon influence region, which are significantly higher than the other regions, ranging from 11 to 23 for lower layer clouds and from 11 to 19 for upper layer clouds. The distributions have patterns similar to the one for total clouds averaged for July, 1983 to December, 1998 derived from ISCCP D2 dataset, which was obtained by averaging eight daily observations; but the measurements are much higher than the previous result that the OD over northwestern China is $1 - 5$[11]. Such distribution characteristics of cloud OD are rather consistent with the distribution of cloud coverage and precipitation over northwestern China[11]. Also, the high-level

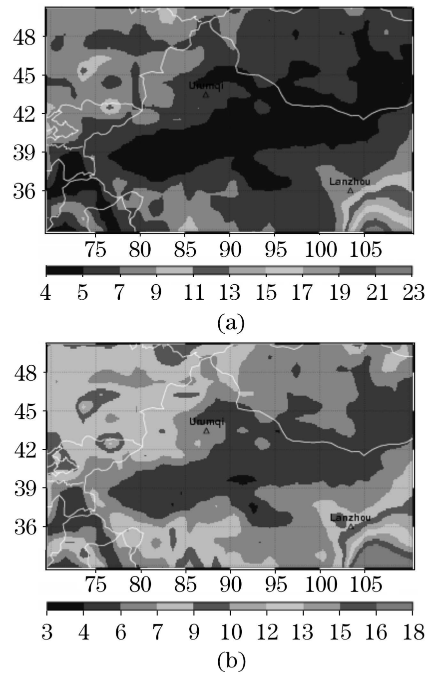

Fig. 1. Distributions of OD for (a) lower layer and (b) upper layer clouds averaged for July 2002 to June 2004.

value areas mentioned above are generally the high value areas of cloud coverage of liquid nimbostratus, ice nimbostratus, deep convective cloud, liquid altostratus, and ice altostratus with high measurements of OD derived from ISCCP D2 data[11].

Usually northwestern China is defined as three regions for the climate research based on general geographic regions. For an enhanced understanding of regional variation in cloud OD, here we define four sub-regions according to geographic and topographic concern: the Asia monsoon influence region with its edge region, Tianshan Mountains, Qilian Mountains, and Taklimakan Desert.

Table 1 indicates that the cloud OD has significant seasonal variation except the desert region. Lower layer clouds in the monsoon region have the highest measurement of OD in autumn which reaches 20.2, and in spring and summer the measurement is quite high also. This region's upper layer cloud OD is actually highest in summer with rather close measurements in spring and

Table 1. Seasonal and Yearly Means of Cloud OD over the Four Regions in Northwestern China

		A	B	C	D
Lower Layer Clouds	Winter	8.5	3.8	2.3	5.0
	Spring	11.6	6.8	6.0	5.1
	Summer	15.3	11.5	12.3	6.1
	Autumn	20.2	6.2	7.6	4.6
	Yearly	13.9	7.1	7.1	5.2
Upper Layer Clouds	Winter	8.4	5.5	5.2	5.3
	Spring	11.4	7.2	7.6	5.0
	Summer	15.4	9.4	9.9	5.8
	Autumn	15.0	7.0	6.7	4.3
	Yearly	12.6	7.3	7.4	5.1

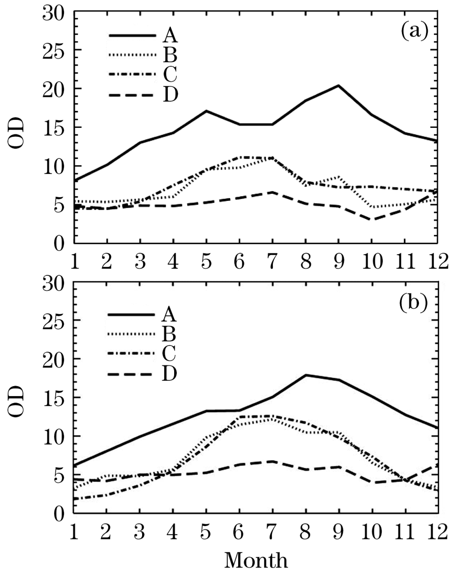

Fig. 2. Illustration of annual cycle of OD over the region A, B, C, and D for (a) lower layer clouds, (b) upper layer clouds. A: the Asia monsoon influence region with its edge region; B: the Qilian Mountains; C: the Tianshan Mountains; D: the Taklimakan Desert.

autumn. The seasonal variation feature of OD is similar to that of cloud coverage, and the high measurement period is consistent with the main precipitation period in this region[11]. In winter the measurements of both lower and upper layer clouds are the lowest of the four seasons. Figures 2(a) and (b) show that OD for the two layer clouds have their apparent peaks during August and September respectively and their lowest dips in January.

The two mountain regions have very similar measurements of OD for all seasons. Winter shows the only notable difference when Tianshan region has less OD in both lower and upper layers of clouds. In fact, the yearly averaged measurements of lower layer cloud are the same and of upper layer are very close. Winter is the season of very low OD for the mountain regions while summer is the season of high OD in the two regions.

As we would suspect, of the four regions, the desert region has the lowest yearly means for OD mainly because of lack of moisture. However, we note that the measurements for lower layer clouds in the desert region are very close to those in the mountain regions in three winter months, and for upper layer clouds are actually higher than in either of the mountain regions in December and January. The two layer clouds in desert region have the highest measurements of OD in summer and the lowest in autumn of all four seasons. The monthly variation curves for both lower and upper layer clouds are of low amplitude, and the peak measurements are in July with close measurements in May and June. Two non-sequential periods of low measurement of OD are found also. One significant low period is in October and the other in February with January being nearly equal (Fig. 2).

From Table 1 we can calculate that the largest differences of yearly means of cloud OD for lower and upper layer clouds, which are 8.7 and 7.5 respectively, occur between the Asia monsoon influence region and the Taklimakan Desert where the largest differences of seasonal means are 15.6 and 10.7 respectively, occurring in autumn.

In summary, the instantaneous measurements of cloud OD presented here are much higher than the previous results derived from ISCCP D2 monthly mean data. The regional variation in cloud OD is quite significant over northwestern China. For an enhanced understanding of seasonal variability of cloud optical property, we should take the sub-regional features into account even for the same climate region.

This work was supported in part by the National Natural Science Foundation of China (No. 40633017 and 40575036) and the National "973" Program of China (No. 2006CB403700). The data were obtained from the NASA Langley Research Center Atmospheric Sciences Data Center. We appreciate Dr. Yuhong Yi for helping us with data and Mr. Jim Miller for smoothing the English. Funding for the processing of the northwestern China data was provided by the Special Professional Outlay for Scientific Research for Commonweal (No. GYHY(QX)2007) and the Shanghai Leading Academic Discipline Project (No. B604). Y. Chen's e-mail address is yonghangchen@yahoo.com.cn.

References

1. K. N. Liou, S. C. Ou, Y. Takano, and J. Cetola, Appl. Opt. **45,** 6849 (2006).
2. Y. Hu, Z. Liu, D. Winker, M. Vaughan, V. Noel, L. Bissonnette, G. Roy, and M. McGill, Opt. Lett. **31,** 1809 (2006).
3. Y. Hu, M. Vaughan, Z. Liu, B. Lin, P. Yang, D. Flittner, B. Hunt, R. Kuehn, J. Huang, D. Wu, S. Rodier, K. Powell, C. Trepte, and D. Winker, Opt. Express **15,** 5327 (2007).
4. Y. Zhang and G. Wang, Chin. Opt. Lett. **4,** 559 (2006).
5. P. Yang and K. N. Liou, J. Opt. Soc. Am. A **14,** 2278 (1997).
6. G. Yuan, X. Sun, and J. Dai, Chin. Opt. Lett. **4,** 425 (2006).
7. P. Minnis, S. Sun-Mack, Y. Chen, H. Yi, J. Huang, L. Nguyen, and M. M. Khaiyer, Proc. SPIE **5979,** 597909 (2005).
8. K. Meyer, P. Yang, and B.-C. Gao, IEEE Geoscience and Remote Sensing Lett. **4,** 471 (2007).
9. Q. Fu and W. B. Sun, J. Quantum Spectro. Rad. Trsnsfer **100,** 137 (2006).
10. S. Yi, H. Liu, W. Li, and Y. Li, J. Meteorology (in Chinese) **29,** 7 (2003).
11. Y. Chen, J. Huang, T. Wang, H. Jin, and J. Ge, J. Appl. Meteorol. Sci. (in Chinese) **16,** 717 (2005).
12. R. Liu, Y. Liu, and B. Du, J. Appl. Meteorol. Sci. (in Chinese) **15,** 468 (2004).
13. S. Ding, G. Shi, and C. Zhao, Chin. Sci. Bull. (in Chinese) **49,** 1105 (2004).
14. Y. Takano and K. N. Liou, J. Atmos. Sci. **46,** 3 (1989).
15. P. Minnis, D. F. Young, D. P. Kratz, J. A. Coakley, Jr., M. D. King, D. P. Garber, P. W. Heck, S. Mayor, and R. F. Arduini, CERES ATBD 4.3, Cloud Optical Property Retrieval (Subsystem4.3), 135 (1997). http://science.larc.nasa.gov/ceres/.
16. P. Minnis, D. Young, S. Sun-Mack, P. W. Heck, D. R. Doelling, and Q. Z. Trepte, Proc. SPIE **5235,** 37 (2003).

17. B. A. Wielicki, B. R. Barkstrom, B. A. Baum, T. P. Charlock, R. N. Green, D. P. Kratz, R. B. Lee, III, P. Minnis, G. L. Smith, T. Wong, D. F. Young, R. D. Cess, J. A. Coakley, Jr., D. A. H. Crommelynck, L. Donner, R. Kandel, M. D. King, A. J. Miller, V. Ramanathan, D. A. Randall, L. L. Stowe, and R. M. Welch, IEEE Trans. Geosci. Remote Sensing **36,** 1127 (1998).
18. G. Tselioudis and W. B. Rossow, Geophys. Res. Lett. **21,** 2211 (1994).
19. G. Hong, P. Yang, B.-C. Gao, B. A. Baum, Y. X. Hu, M. D. King, and S. Platnick, J. Appl. Meteorol. Climatol. **46,** 1840 (2007).
20. M. H. Zhang, W. Y. Lin, S. A. Klein, J. T. Bacmeister, S. Bony, R. T. Cederwall, A. D. Del Genio, J. J. Hack, N. G. Loeb, U. Lohmann, P. Minnis, I. Musat, R. Pincus, P. Stier, M. J. Suarez, M. J. Webb, J. B. Wu, S. C. Xie, M.-S. Yao, and J. H. Zhang, J. Geophys. Res. **110,** D15S02 (2005).